Arabian Journal of Chemistry (2021) **14**, 103040

King Saud University

Arabian Journal of Chemistry

www.ksu.edu.sa
www.sciencedirect.com

ORIGINAL ARTICLE

Capillary column inverse gas chromatography to determine the thermodynamic parameters of binary solvent poly (styrene-block-butadiene) rubber systems

Hassiba Benguergoura [a], Amina Allel [b], Waseem Sharaf Saeed [c], Taïeb Aouak [c,*]

[a] *Laboratoire de chimie-physique moléculaire et macromoléculaire LCPMM, Faculté des Sciences, Département de Chimie, Université Saâd Dahlab Blida 1, Route de Soumâa, B. P. 270, Blida 09000, Algeria*
[b] *Faculté de Technologie, Département de Chimie Industrielle, Université Saâd Dahlab Blida 1, Route de Soumâa, B. P. 270, Blida 09000, Algeria*
[c] *Chemistry Department, King Saud University, PO Box 2455, Riyadh 11451, Saudi Arabia*

Received 10 November 2020; accepted 20 January 2021
Available online 3 February 2021

KEYWORDS

Inverse gas chromatography;
Capillary column;
Poly(styrene-block-butadiene) rubber;
Thermodynamic parameters;
Nonrandom two-liquid model;
Universal quasichemical model

Abstract Capillary column inverse gas chromatography (CCIGC) was adapted to determine the thermodynamic properties of poly (styrene-co-butadiene) rubber (SBR) and various molecules, including aliphatic alkanes (C6, C7 and C8), alicyclics (C5 and C6)), aromatics (benzene and toluene), ethanol, tetrahydrofuran and acetonitrile. Capillary column inverse gas chromatography (CCIGC) was adapted to determine the thermodynamic properties of poly (styrene-co-butadiene) rubber (SBR) and various molecules, including aliphatic alkanes (C6, C7 and C8), alicyclics (C5 and C6)), aromatics (benzene and toluene), ethanol, tetrahydrofuran and acetonitrile. The results obtained were compared with those of the literature determined by packed column (PCIGC) and by other methods. It was revealed that the values of the heat of vaporization and the Hansen solubility parameter determined by CCIGC in some cases agree well with those of the literature, while in other cases deviates significantly. The comparison of the values of the literature obtained by PCIGC determined by different authors, significant differences were also observed in certain cases. This gap is undoubtedly related to the experimental errors occurred during the support treatment

* Corresponding author.
E-mail addresses: amina.allel@univ-blida.dz (A. Allel), wsaeed@ksu.edu.sa (W. Sharaf Saeed), taouak@ksu.edu.sa (T. Aouak).
Peer review under responsibility of King Saud University.

Production and hosting by Elsevier

https://doi.org/10.1016/j.arabjc.2021.103040

and/or during the preparation of the column. The activity coefficients of the solvents at infinite dilution were calculated and compared with those obtained by fitting the non-random two-liquid and universal quasichemical models.

1. Introduction

The compatibility of polymer–solvent systems is extremely important for determining the suitability of a polymer for a given application. The widely used model for studying polymers in solutions is based on the Flory–Huggins theory (Flory, 1941), where the main objective is to estimate the polymer–solvent interaction parameter, χ. This unit-less entity is used to characterize the thermodynamic state of a mixture of a polymer and solvent or another polymer. In all cases, the interaction between a polymer and another compound plays a significant role (Horta and Pastoriza, 2005).

The determination of interaction parameters has been a subject of extensive research. For "solvent–polymer" systems, a large number of techniques and parameters, including the vapor pressure of the solvent, osmotic pressure, equilibrium of sedimentation, diffraction of light at small and large angles, and swelling (Flory, 1941) and inverse gas chromatography (IGC) are employed to determine these interaction parameters (Mohammadi-Jam and Waters, 2014; Voelkel et al., 2009). IGC is among the most efficient techniques for estimating the thermodynamic properties of polymers, solvents, and polymer–solvent and polymer–polymer systems. Additionally, ICG is regarded as the simplest, fastest, and most precise technique to perform physicochemical measurements on various non-volatile materials in different forms and morphologies, including modified silica, glass fibers, and certain pharmaceutical products in the form of powders (Conder and Young, 1979). However, IGC is the preferred technique for polymers and has a wide range of applications (Mohammadi-Jam and Waters, 2014). ICG allows the rapid and precise estimation of the Hansen solubility parameters for solvents and polymers and for polymer–solvent and polymer–polymer systems. Moreover, IGC has been used to determine various other polymer properties, such as the glass-transition temperature, degree of crystallinity, activity coefficients, and adsorption isotherms (Guillet and Al-Saigh, 2006). In our previous work, we used IGC to validate pervaporation results (Hadj-Ziane et al., 2005; Moulay et al., 2006).

IGC can be performed in two different modes: (1) infinite dilution (where Henry's law is valid) and (2) finite concentration. IGC at infinite dilution (IGC ID) involves injecting very small quantities of probe molecules (at the limit of detection) to neglect interactions between the adsorbed molecules (Voelkel et al., 2009). IGC ID allows the determination of the thermodynamic quantities of the interactions developed between the polymer and molecules with which it is brought into contact. Therefore, ICG is among the simplest techniques for measuring the solubility and diffusivity of polymer systems with ID and polymer systems using filled and capillary columns. However, the filled-column model, which was initially employed by Gray and Guillet (Gray and Guillet, 1973), has the following disadvantage: non uniform distribution of polymer; moreover, the contribution of the factor linked to the adsorption of the support is not always negligible. Consequently, this method yields less-precise values for evaluating diffusion coefficients and sorption. As a result, the reported values of the intrinsic thermodynamic parameters related to a same solute in terms of the vaporization heat and solubility parameter determined by packed-column IGC (PCIGC) using different stationary phases sometimes differ (Cai et al., 2002; Diez et al., 2011; DiPaola-Baranyi, 1982; Hadj-Ziane et al., 2005; Ugraskan et al., 2020). This is mostly due to the effect of the adsorption of the support. To minimize this effect, the support must be perfectly inert and uniformly impregnated by the stationary phase.

However, taking into account the phenomenon of friction between the impregnated particles during the preparation of the column and the filling of the column, the minimization of errors in the determination of the weight of polymer in the column is not always ensured.

However, given the friction phenomenon between the impregnated particles during column preparation and column filling, the minimization of errors in the determination of the weight of polymer inside the column is not guaranteed every time. Moreover, such effects have been highlighted during the determination of the Flory–Huggins interaction parameters involving miscible blends using PCIGC. Indeed, it was revealed that the Flory–Huggins parameters vary according to the nature of the probe molecule (Al-Ghait et al., 2012; Etxeberria et al., 1994; Huang, 2006), but in principle, this should not be assumed. In such a case, if this occurs, it is only because of the phenomenon of adsorption linked to the support. Indeed, the adsorption of the support depends on the nature of the adsorbed probe molecule; therefore, its effect is projected on the values of these parameters. Using a capillary column in which the polymer is more uniformly deposited on the walls of the column, Pawlisch *et al.* (Pawlisch et al., 1988; Pawlisch et al., 1987) proposed a more precise method for measuring these coefficients. Since then, capillary column IGC (CCIGC) has frequently been employed to study the transport and thermodynamic properties of polymer–solvent systems with ID (Balashova et al., 2001; Cai et al., 2002; Huang, 2006; Huang, 2004). The principle of this technique is based on the distribution of the volatile solvent between the gaseous mobile phase and stationary phase comprising the polymer. The most important factor is to determine the partition coefficient, K_P, which is the ratio of the concentration of the solvent in the polymer phase to that of the solvent in the vapor phase.

Poly(styrene-*co*-butadiene) rubber (SBR) is an elastomer that exhibits excellent chemical, thermal, and mechanical stabilities. These properties enable SBR to be widely used in the rubber industry as latex for rubber adhesives and supports for carpets, belts, floor coverings, wires, and cables for installations (Chahal et al., 2012). Therefore, the knowledge of the

thermodynamic properties of the SBR solution undoubtedly make it suitable for applications in other fields.

The contributions of this study include the importance of CCIGC for determining the thermodynamic properties of polymers and solvents and to minimize the experimental errors mainly due to the support treatment and/or column preparation used in the PCIGC method. In this work the CCICG technique is applied to estimate the solubility parameters of solvents and SBR. To achieve these objectives, a capillary column that was covered on its inside surface with a thin layer of SBR as the stationary phase was prepared via the casting method. This column was used to estimate the retention volumes of the solvents used as probes, the activity coefficients, polymer–solvent interactions, and solubility parameters of the copolymer and solvents were determined at different temperatures.

2. Materials and methods

2.1. Materials

SBR ($\bar{M}n = 6.0{\cdot}10^5$ g•mol^{-1}) containing 45% styrene, cyclopentane (97% purity), toluene (99.5% purity), and ethanol (99.9% purity) was supplied by Sigma-Aldrich (Munich, Germany). *n*-Octane, *n*-heptane, acetonitrile, benzene, tetrahydrofuran (THF), and propanol were purchased from Panreaca Quimica SA (Barcelona, Spain). *n*-Hexane (99% purity) and cyclohexane (99% purity) were provided by Fluka (Buchs, Switzerland). All chemicals were used without further purification.

2.2. Characterization

Knowing the thermal properties, such as the glass-transition, melting, and degradation temperatures, of the polymer constituting the stationary phase is essential in the chromatography domain because these parameters determine the limit under which the column can be conditioned and used. We previously investigated the thermal properties of SBR via differential scanning calorimetry (DSC) and thermogravimetric analysis (TGA) (Benguergoura and Moulay, 2012). The profile of the DSC chromatogram of the terpolymer revealed that the glass-transition temperature, T_g, and melting temperature, T_m, were −55 °C and 246 °C, respectively, and its thermal decomposition, as determined by the TGA, started at 375 °C.

The uniformity of the internal coating and average film thickness were estimated by scanning electron microscopy (SEM) analyses using a JSM-6060LV microscope (JEOL, Tokyo, Japan), and the samples were coated with a gold grid.

2.3. Column preparation

A Supelco-type capillary column comprising fused silica of intermediate polarity (internal diameter, 0.35 mm; length, 30 m) was filled with 0.2 w/v% solution of SBR using a syringe pump according to a previously described dynamic filling procedure (Ugraskan et al., 2020). The column was maintained at a constant temperature by placing it in an oven specially modified for the purpose of allowing the solvent to slowly evaporate and form a uniform coating.

Fig. 1 shows the micrographs of the cross-sections of a virgin and SBR-coated capillary column. The cross-section of the SBR-coated capillary column showed a thin additional layer of SBR with a thickness varying between 1.53 and 1.64 µm according to the measurements of different sections, thus revealing that the capillary column was successfully prepared. Similar thickness is usually used in IGC (Bonifaci et al., 1994; Tihminlioglu and Danner, 1999).

Prior to use, the column was conditioned at 250 °C under a slow carrier-gas flow for 24 h. The flow rate (4 mL•min^{-1}) was controlled with a soap-bubble flowmeter for all the probes injected at room temperature (~25 °C).

2.4. Retention volume measurements

We used a gas chromatograph-type 17A column (Shimadzu, Kyoto, Japan) equipped with a flame ionization detector to measure the retention volume. Injection was performed using a 5-µL Hamilton syringe (Hamilton, Reno, NV, USA) and 1.0 µL of each molecular probe in its vapor state for each analysis, and the experiment was conducted thrice for each solvent and temperature combination. The arithmetic average of the retention times of the repeated injections (with errors of ± 0.1 min) was used to calculate the retention volume. The net retention volume, V_N, was calculated from the collected retention times of the studied probes using the following equation (Ugraskan et al., 2020):

$$V_N = Q \cdot j_3^2 \left(\frac{T}{T_f}\right)(t_R - t_m), \tag{1}$$

where t_R and t_m are the retention time of the molecular probe and the retention time of methane, which was used as the non-retained gas (marker gas), respectively. The $t_N$value was measured for all molecular probes at 30 °C, 40 °C, 50 °C, 60 °C, and 70 °C. Additionally, Q is the flow rate measured at the column outlet using a soap-bubble flowmeter at temperature T_f, T is the column temperature, and j_3^2 is the James–Martin gas-compressibility correction factor [Eq. (2)] (James and Martin, 1952):

$$j_3^2 = \frac{3}{2}\left[\frac{\left(\frac{P_i}{P_o}\right)^2 - 1}{\left(\frac{P_i}{P_o}\right)^3 - 1}\right], \tag{2}$$

where P_i and P_o are the pressure at the inlet and outlet of the column, respectively.

The specific retention volume is vital in the calculation of thermodynamic parameters. For all molecular probes, the specific retention volume was calculated using Eq. (3), as adapted from Yampolskii et al. (Yampolskii and Belov, 2015) on the basis of the Davankov works (Domínguez et al., 2001), which was taken as the basis for novel official IUPAC recommendations:

$$V_g^{273} = \frac{273.15}{T}\frac{V_N}{w_S}, \tag{3}$$

where w_S is the mass of the polymer and T is the column temperature. The retention time can be determined either from the maximum peak time, or from the first moment of the peak. According to various previous studies (Balashova et al., 2012; Davis et al., 2004; Eser and Tihminlioglu, 2005), both the methods yield precise values with regards to the thermody-

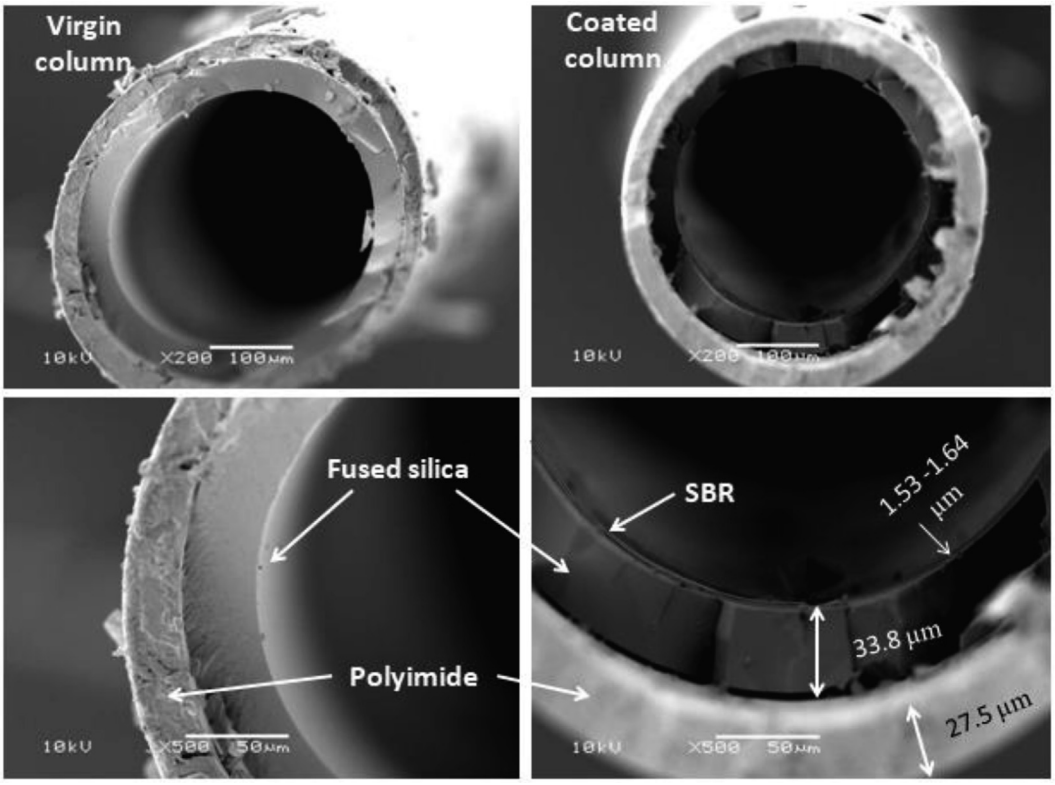

Fig. 1 SEM micrographs of cross-sections of a virgin and SBR-coated capillary column.

namic or transport properties for polymer–solvent systems. Several models exist for estimating the retention time.

The retention time can be determined either from the top of the peak or its first appearance in the chromatogram. According to previous studies (Balashova et al., 2012; Davis et al., 2004; Eser and Tihminlioglu, 2005), both methods yield precise values with regard to thermodynamic or transport properties for polymer–solvent systems. Several models exist for estimating the retention time based on the mathematical processing of elution data that correspond to the chromatographic peak of a theoretical concentration profile, generally by means of the Laplace transform. The simplest method is that employing the distribution of retention times by analogy with the distribution of the residence-time [Eq. (4)] and the partition coefficient, K_p, expressed by Eq. (4) (Balashova et al., 2012), which is the ratio of the concentration of the solvent in the polymer phase to that of the solvent in the gas phase.

$$\mu_K = \frac{\int_0^\infty \mathrm{t_k} C(t)dt}{\int_0^\infty C(t)dt}, \tag{4}$$

$$K_P = \left(\frac{r(\mu_1 - 1)}{2\epsilon}\right) t_m, \tag{5}$$

where r is the radius of the capillary column, ε is the thickness of the polymer film on the internal wall of the column, t_m is the retention time of the inert gas, and μ_1 is the start time of the peak. The specific retention volume is also related to the partition coefficient by the Laub and Pecsok equation [Eq. (6)] (Laub and Pecsok, 1978):

$$V_g^{273} = \frac{273,15}{T}\frac{K_p}{\rho_p}, \tag{6}$$

where T (K) is the column temperature. Moreover, ρ_p is the density of the polymer at the temperature of the column. For small intervals of temperature and at constant pressure, the density of the polymer at temperature T is calculated using Eq. (7):

$$\rho_p = \frac{\rho_p^o}{1 + 3\alpha(T - T_o)}, \tag{7}$$

where ρ_p^o is the density of the polymer measured at temperature T_o and α is the linear thermal expansion coefficient, which is $5.8{\cdot}10^{-6}$ °C^{-1} for SBR (Kim et al., 2019). The specific retention volume varies with temperature. In the absence of any change in the physical state and/or modification of the structure of the stationary phase, the plot of $ln\left(V_g^{273}\right)$ versus the inverse of the temperature (the retention diagram) is a straight line. Before the T_g value, the linearity presumes sorption equilibrium in the mass of the polymer, and the molar heat of sorption $\Delta H_{S(i)}$ is deducted from the slope of the curve using the following equation (Farshchi et al., 2018):

$$\Delta \mathrm{H}_{S(i)} = -\frac{R\ \partial ln \mathrm{V}_\mathrm{g}^{273}}{\partial\left(\frac{1}{T}\right)}, \tag{8}$$

where R is the gas constant.

Beyond T_g + ~20 °C, as in the case of SBR (T_g = −55 °C), the linearity presumes the dissolution equilibrium of the solvent in the polymer, whose heat of dissolution, ΔH_{diss}, is

directly deduced from the slope of the straight line, as expressed by Eq. (9):

$$\Delta H_{\text{diss}} = -\frac{R\ \partial ln V_g^{273}}{\partial\left(\frac{1}{T}\right)}, \tag{9}$$

2.5. Determination of the weight-fraction activity coefficient

According to Braum and Guillet (Gray and Guillet, 1973), the weight-fraction activity coefficient at infinite dilution, Ω_1^∞, is expressed by Eq. (10):

$$\Omega_1^\infty = \frac{RT}{P_1^0 V_g^{273} M_1} exp\left[-\frac{P_1^0}{RT}\left(B_{11} - V_1^o\right)\right], \tag{10}$$

where V_1^o and M_1 are the molar volume and molar mass of the solvent, respectively, P_1^o is the vapor pressure calculated from the Antoine equation [Eq. (11)] (Boublík et al., 1984), and T is the temperature of the system.

$$\ln P_1^o(\text{KPa}) = \text{A} - \frac{\text{B}}{\text{T}(^\circ\text{C}) + \text{C}}, \tag{11}$$

where A, B, and C are Antoine's constants and B_{11} is the second Virial coefficient. Voelkel and Fall (Voelkel and Fall, 1995) revealed that there is a significant change in the interaction parameter when the second coefficient of Virial is changed. The latter can be obtained from the Guggenheim and Wormald relationship (Guggenheim and Wormald, 1965), which is expressed as follows:

$$\frac{B_{11}}{V^c} = 0,500 - 1,144\left(\frac{T^c}{T}\right) - 0,480\left(\frac{T^c}{T}\right)^2 - 0,042\left(\frac{T^c}{T}\right)^3, \tag{12}$$

where V^c, T, and T^c are the critical volume, temperature of the experiment, and critical temperature, respectively. The value of Ω_1^∞ characterizes the polymer–solvent compatibility. According to Farshchi *et al.* (Farshchi et al., 2018), a Ω_1^∞value < 5 indicates good solvation, a value between 5 and 10 indicates moderate solvation, and a value > 10 implies poor solvation.

2.6. Determination of the Flory–Huggins interaction parameters

The Flory–Huggins interaction parameter, $\chi_{1,p}$, is used to measure the strength of interactions and, therefore, as a guide in the prediction of polymer–solvent compatibility. According to Gray and Guillet (Gray and Guillet, 1973), this parameter is related to the weight-fraction activity coefficient as follows:

$$\chi_{1,p} = ln\Omega_1^\infty + ln\left(\frac{\rho_1}{\rho_p}\right) - \left(1 - \frac{1}{r_s}\right), \tag{13}$$

where r_s is the number of segments in the polymer chain, which is calculated as follows:

$$r_s = \frac{\rho_1 M_p}{\rho_p M_1}, \tag{14}$$

where ρ_1 is the density of the solvent and M_1 and M_p are the molecular weights of the solvent and the polymer, respectively.

Theoretically, the Flory interaction parameter decreases with increasing temperature (Flory, 1941). For a polymer–solvent binary system, the χ parameter is the sum of the two contributions depending on the temperature, the entropic parameter related to the free volume of the solvent (which increases with temperature), and the enthalpic parameter related to the intermolecular forces between the polymer and solvent (which decreases with temperature). Therefore, the overall dependence is determined by the predominant effect (Diez et al., 2011). According to the Flory–Huggins theory, a polymer is soluble in a given solvent if the $\chi_{1,p}$value of such a system is < 0.5 (Balashova et al., 2012), and it becomes more soluble as this parameter approaches zero. For a $\chi_{1,p}$ close to 0.5, the polymer is only soluble in the solvent at a certain temperature (called θ-temperature), and such a solvent is called θ-solvent.

2.7. Determination of solubility parameters

2.7.1. Solubility parameters of solvents

The solubility parameter,δ_i, of a compound, i, is related to the square root of the cohesion energy of i, $E_{v(i)}$, which is also related to the heat of vaporization of i. δ_i is then calculated as follows (Zhu et al., 2019):

$$\delta_i = \left(\frac{\Delta E_{v(i)}}{V_i}\right)^{0.5} = \left[\frac{\Delta H_{vap(i)} - RT}{V_i}\right]^{0,5}, \tag{15}$$

where V_i is the molar volume of i, where its variation is practically negligible in the temperature range of 30 °C to 70 °C. From the value of the activity coefficient determined at a given temperature, $\Delta H_{vap(i)}$ of the solvent i is calculated as follows:

$$\Delta H_{vap(i)} = \Delta H^\infty_{mix(i)} - \Delta H_{diss(i)}, \tag{16}$$

where $\Delta H_{diss(i)}$ is the heat of disolution of solvent i, which is calculated using Eq. (9), and $\Delta H^\infty_{mix(i)}$is the partial molar heat of solvent i in the mixture, which is calculated from Eq. (17) (Farshchi et al., 2018).

$$\Delta H^\infty_{\text{mix(i)}} = \text{R}\left[\frac{\partial(\ln(\Omega_1^\infty)}{\partial(1/\text{T})}\right], \tag{17}$$

The data used to determine the different thermodynamic parameters adapted from the literature are listed in Table 1.

2.7.2. Solubility parameter of SBR

According to the Flory–Huggins theory modified by Blanks and Prausnitz (Blanks and Prausnitz, 1964), the interaction parameter,$\chi_{1,p}$, can be calculated from the difference between the solubility parameter of the solvent, δ_1, and that of the polymer,δ_p, according to the following equation:

$$\chi_{1,p} = \beta + \frac{V_1}{RT}(\delta_1 - \delta_p)^2, \tag{18}$$

where β is the entropic factor most often equal to 0.34 (Marzocca, 2007). According to Di Paola-Baranyl and Guillet (DiPaola-Baranyi, G., 1982), the rearrangement of this equation as follows:

$$\frac{\delta_1^2}{2} - \frac{RT\chi_{1,p}}{2V_1} = \delta_1\delta_2 - \left(\frac{\delta_p^2}{2} + \frac{0.34RT}{2V_1}\right), \tag{19}$$

This gives access to the polymer-solubility parameter,δ_P, which can be easily determined from the slope and intercept at the experimental temperature of the curve, indicating the variation of the left-hand side of this equation versus δ_1.

Table 1 Data used in the determination of the different thermodynamic parameters adapted from literature.

	ρ_1(g•ml^{-1})[a]	V_1[a] (cm^3•mol^{-1})	M_1[a] (g•mol^{-1})	B_{11}[b]				
Temperature (°C)				30	40	50	60	70
n-Hexane	0.654	131.76	86.17	−12.37	−11.68	−11.05	−10.47	−9.94
n-Heptane	0.684	146.49	100.20	−13.68	−12.98	−12.22	−11.58	−11.00
n-Octane	0.703	162.49	114.23	15.13	−14.29	−13.53	−12.82	−12.17
Cyclopentane	0.751	93.38	70.13	−10.81	−10.21	−9.66	−9.15	−8.68
Cyclohexane	0.779	108.03	84.15	−12.25	−11.57	−10.95	−10.38	−9.85
Benzene	0.879	89.17	78.11	−11.28	−10.65	−10.08	−9.55	−9.07
Toluene	0.866	106.39	92.13	−12.93	−12.21	−11.56	−10.95	−10.4
THF	0.889	81.11	72.10	−9.96	−9.41	−8.90	−8.43	−8.01
Methanol	0.791	40.50	32.04	−10.77	−10.17	−9.12	−9.12	−8.65
Ethanol	0.789	58.38	46.06	−10.65	−10.06	−9.51	−9.02	−8.56
Propanol	0.803	74.83	58.07	−11.56	−10.92	−10.33	−9.79	−9.29
Acetonitrile	0.786	52.23	41.05	−13.76	−12.99	−12.29	−11.65	−11.06

[a] Taken from the literature: R.H. Perry, D.W. Green, J.O. Maloney, *Perry's Chemical Engineers Handbook*, McGraw-Hill, 6th edition, New York, 1984.
[b] Calculated from Eq. (12).

Table 2 Specific retention volumes of probes obtained at different temperatures.

Solvent	$V_g^o(cm^3/g)$				
	30 °C	40 °C	50 °C	60 °C	70 °C
n-Hexane	133.72	91.29	63.93	44.70	32.27
n-Heptane	199.51	132.23	83.08	58.89	40.94
n-Octane	184.27	119.87	79.47	53.82	37.31
Cyclopentane	311.93	207.38	135.13	94.85	65.60
Cyclohexane	276.26	188.26	120.26	81.57	54.99
Benzene	311.27	210.02	146.55	105.93	76.84
Toluene	335.38	220.55	147.19	107.64	79.19
Ethanol	13.80	10.96	11.64	11.09	11.80
THF	332.36	200.74	131.47	87.46	60.96
Acetonitrile	24.48	17.58	13.26	10.40	8.33

3. Results and discussion

3.1. Determination of thermodynamic parameters

The specific retention volume, V_g^{273}, of each of the investigated solvents was calculated from the retention time at 30 °C, 40 °C, 50 °C, 60 °C, and 70 °C, which are remarkably higher than the T_g obtained from the top of the chromatogram peak and Eq. (3). The results obtained are listed in Table 2. Additionally, we determined the V_g^{273} of the solvents using the first moment of the elution peak, with similar results obtained with an error percentage of < 3%. The reported values of V_g^{273} refer to the average of the three measurements. In all cases, the standard deviation did not exceed 2.0% of the reported value. As shown in Table 1, the $V_g^{273}$of each molecular probe decreased as the temperature increased.

We then calculated the activity coefficient at ID of solvent Ω_1^∞ from the V_g^{273} values at the same temperatures using Eq. (10) (Table 3). The data revealed that the weight-fraction activity coefficient varied along with temperature and depending on the nature of the molecular probe. Furthermore, the Ω_1^∞ of the alkanes slowly fluctuated, whereas those of the aromatics and acetonitrile slowly decreased, that of ethanol significantly decreased, and that of THF slowly increased. This could be attributed to the polarity of the molecular probes; the Ω_1^∞ of ethanol was reduced by ~ 4-fold due to its high polarity. These findings were expected, given that increases in temperature reduces the repulsive interactions between the polymers, nonpolar (SBR), and polar (ethanol) molecules. This is explained by the $\chi_{1,p}$values of this system presented in the following section.

As shown in Table 3, the values of Ω_1^∞ for polar solvents, such as ethanol and acetonitrile, were higher than those of nonpolar solvents, indicating their incompatibility with regard to the SBR copolymer. Toluene, which has the lowest Ω_1^∞ value, represents the best solvent for this copolymer. Importantly, note that the parameter is strongly dependent on temperature in the case of non polar and weakly-polar solvents.

This observation agrees with that reported by Balashova et al. (Balashova et al., 2001). However, ethanol, which has the highest polarity among all of the probes, is usually used as a precipitant for SBR; its Ω_1^∞ dramatically decreases when the temperature increases. This phenomenon is attributed to the fact that an increase in the temperature of the ethanol–SBR mixture weakens the strong repulsive forces between

Table 3 Activity coefficient at infinite dilution, Ω_1^{∞} obtained at different temperatures.

Solvent	Ω_1^{∞}				
	30 °C	40 °C	50 °C	60 °C	70 °C
n-Hexane	7.23	7.16	7.12	7.28	7.38
n-Heptane	7.63	7.56	8.15	8.01	8.22
n-Octane	8.26	8.34	8.52	8.76	9.02
Cyclopentane	4.88	4.82	5.01	4.97	5.13
Cyclohexane	5.51	5.31	5.63	5.78	6.12
Benzene	4.89	4.76	4.62	4.45	4.38
Toluene	4.54	4.53	4.60	4.38	4.25
Ethanol	110.30	91.23	58.19	42.53	28.52
THF	4.58	4.98	5.15	5.39	5.52
Acetonitrile	62.18	56.85	51.07	45.32	40.38

Table 4 Flory-Huggins interaction parameters of the SBR–solvent systems at different temperatures.

Solvent	$\chi_{1,p}$				
	30 °C	40 °C	50 °C	60 °C	70 °C
n-Hexane	0.59	0.58	0.57	0.59	0.61
n-Heptane	0.68	0.67	0.75	0.73	0.76
n-Octane	0.79	0.80	0.82	0.85	0.88
Cyclopentane	0.33	0.32	0.36	0.35	0.38
Cyclohexane	0.31	0.28	0.33	0.36	0.42
Benzene	0.49	0.46	0.43	0.39	0.38
Toluene	0.40	0.40	0.41	0.37	0.33
Ethanol	3.50	3.31	2.86	2.54	2.14
Tetrahydrofurane	0.44	0.52	0.55	0.60	0.62
Acetonitrile	2.92	2.83	2.72	2.60	2.49

the hydroxyl group of ethanol and the alkyl groups of the macromolecular segments.

3.1.1. Effect of temperature on the Flory interaction parameters

The $\chi_{1,p}$ values calculated in this study using Eq. (13) are summarized in Table 4. As expected, these results were consistent with those of Ω_1^{∞} (Table 3), as they are closely and proportionally related to $\chi_{1,p}$ according to Eq. (13). $\chi_{1,p}$ well translates the extent of polymer–solvent affinity, as its smaller value translates to greater compatibility. For example, the $\chi_{1,p}$ for a SBR/-toluene system agrees with that reported by previous studies and determined using other techniques (0.38–0.41) (Abd-El-Messieh and Abd-El-Nour, 2003; Cho et al., 2000; George et al., 1999; Scuracchio et al., 2004; Traeger and Castonguay, 1966). The $\chi_{1,p}$ for SBR–solvent systems involving cyclohexane, cyclopentane, toluene, and THF range from 0.31 to 0.44, thus revealing moderate affinity for SBR at practically all investigated temperatures. Benzene is considered an θ-solvent; however, ethanol and acetonitrile, having an $\chi_{1,p}$ largely > 0.5 at all the investigated temperatures, are considered precipitants. *n*-Hexane and *n*-heptane are considered non-solvents.

3.1.2. Effect of the molar mass of the molecular probe on the Flory interaction parameters

Fig. 2 shows the variation in the Flory interaction parameter according to the molar mass and carbon number of the molecular probes. Furthermore, Fig. 2 shows that $\chi_{1,p}$ increases along with the molar mass of the probe. Additionally, solvents containing the same carbon number, both aromatic and cyclic, are more compatible with the polymer.

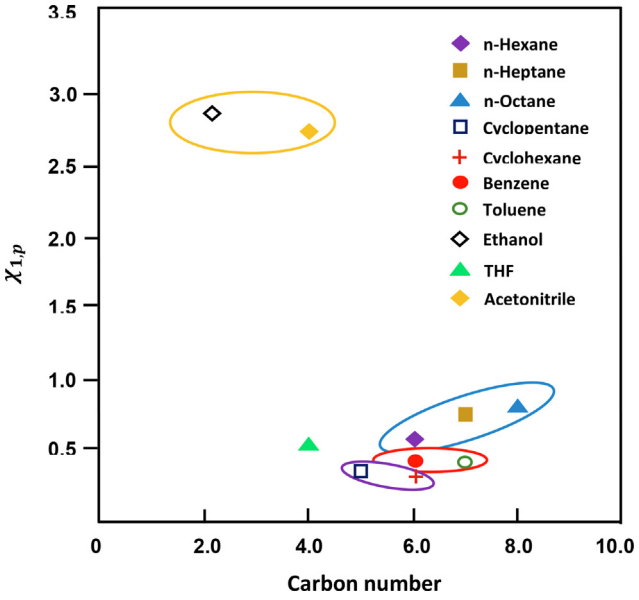

Fig. 2 Variation in the Flory interaction parameter according to the molar mass and carbon number of the molecular probes.

3.1.3. Determination of solubility parameters

We calculated the Hildebrand and Scott solubility parameter of each compound using Eq. (15) and the corresponding heat of vaporization. $\Delta H_{vap(i)}$ is obtained from $\Delta H_{diss(i)}$ and $\Delta H^{\infty}_{mix(i)}$, which are deducted from the slope of the plots of LnV^{o}_{g} and $Ln\ \Omega^{\infty}_{1}$ versus the inverse of temperature, respectively (Figs. 3 and 4). For all of the volatile compounds investigated, $\Delta H_{diss(i)}$, $\Delta H^{\infty}_{mix(i)}$, and $\Delta H_{vap(i)}$ were obtained with an $R^2 > 0.9$. For comparison, Table 5 lists the different heats obtained in this study and the enthalpy of vaporization of similar organic molecules reported previously (Diez et al., 2011) and those calculated from the Watson model (Watson, 1943).

We obtained $\Delta H_{diss(i)}$ and $\Delta H_{mix(i)}$ values over a temperature range of 30 °C to 70 °C. The results reveal that the exothermic molar enthalpy of sorption for the aliphatic and aromatic hydrocarbons increased along with the chain length, indicating that hydrocarbons with the highest number of carbon atoms were better appreciated by the copolymer. However, the molar heat of sorption of the probes was directly affected by the polarity and chemical structure of the probe. Therefore, ethanol, which has the highest polarity among the investigated molecules, was minimally appreciated by SBR. Moreover, for the SBR/THF system, the $\Delta H_{mix(i)}$ was highly exothermic, indicating that THF exhibits strong interactions with SBR.

Furthermore, Table 5 shows that the $\Delta H_{v(i)}$ for all of the probes was generally comparable with those previously reported (Daubert and Danner, 1985; Diez et al., 2011; Dritsas et al., 2008), which were determined by PCIGC and confirmed by those calculated through the Waston approach (Watson, 1943). However, the difference between the different $\Delta H_{v(i)}$ values obtained through the PCIGC method (although minimal in certain cases) is mainly attributed to the experimental errors occurred during the support traitment and/or the column preparation.

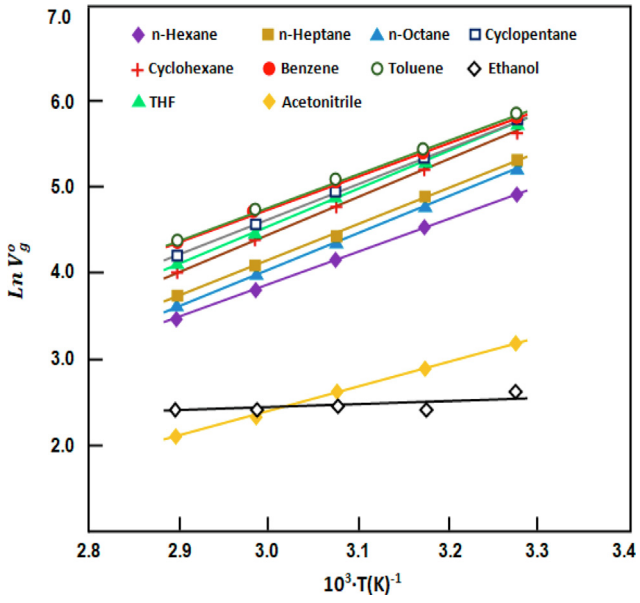

Fig. 3 Variation in LnV^{o}_{g} versus the inverse of temperature for different solvent–SBR binary systems.

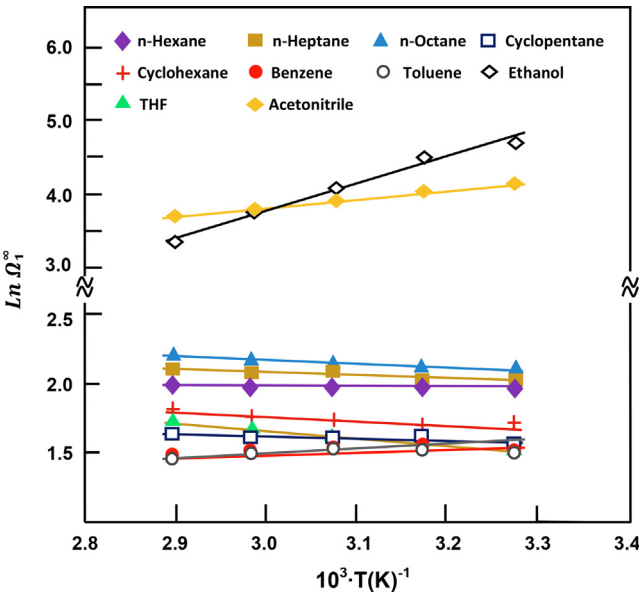

Fig. 4 Variation in $Ln\Omega^{\infty}_{i}$ versus the inverse of temperature for different solvent–SBR binary systems.

To verify this, it is possible to compare the values of $\Delta H_{v(i)}$ determined by PCIGC. Indeed, the presence of a significant gap in the heat of vaporization in certain cases, such as acetonitrile (2.3 KJ·mol^{-1}), ethanol (1.9 KJ·mol^{-1}), THF (1.1 KJ·mol^{-1}), and n-octane (1.1 KJ·mol^{-1}), is closely related to treatment of the support and column preparation. In many cases, controlling the complete coverage and inert character of the support particles is difficult. Table 6 shows the δ_i values obtained from Eq. (15) and those determined previously using PCIGC and other techniques (viscosimetry and swelling methods). To confirm these findings, it will be necessary to compare the results obtained in the present study with those obtained using the same technique (CCIGC) but employing stationary phases other than SBR. Currently, the absence of such studies precludes a comparison here.

It is important to underline here, that the experimental errors have nothing to do with the method itself, on the contrary according to Braum and Gillet (Braum and Gillet, 1975) the PCIGC technique seems to be more adapted to this kind of work. Here we only report those experimental errors that can be made person to person in the stages of column preparation when it is a packed column.

These results indicated that the δ_1 values determined for certain solvents, such as n-hexane, cyclohexane, benzene, toluene, THF, and acetonitrile, generally agreed well with those previously reported and determined by PCIGC and viscosimetry and swelling techniques (Koenhen and smolders, 1975; Scott and Magat, 1949; Hansen, 1967). However, anomalies in these values were also observed, despite use of PCIGC to determine certain solubility parameters, such as those provided by Sreekanth (Sreekanth et al., 2012), Lim (Lim et al., 2014), and Sreekanth and Reddy (Sreekanth and Reddy, 2008). In these cases, these values were relatively underestimated. These anomalies appeared to be a consequence of different factors, including imperfect treatment of support and column preparation. Because, insufficient treatment leads to adsorption of the probe molecule by the support

Table 5 Different enthalpic parameters of solutes estimated in the temperature range of 30–70 °C and those obtained by the packed column inverse gas chromatograph (PCIGC) and Watson approach.

Solvent	$\Delta H_{diss(i)}$ (KJ.mol^{-1})	$\Delta H_{mix(i)}$ (KJ.mol^{-1})	$\Delta H_{vap(i)}$(KJ.mol^{-1})		
			This work	PCIGC	Watson model[f]
n-Hexane	−31.16	−0.80	30.36 ± 0.20	29.9[a]; 29.5[b]	31.3
n-Heptane	−34.85	−1.76	33.09 ± 0.22	35.5[a]; 34.6[b]	36.2
n-Octane	−35.00	−0.89	34.11 ± 0.18	40.4[a]; 39.3[b]	40.9
Cyclopentane	−34.17	−2.15	32.02 ± 0.23	27.7[a]; 28.0[c]	28.0
Cyclohexane	−35.58	−3.44	32.13 ± 0.22	31.1[a]; 32.0[c]	32.1
Benzene	−30.52	2.52	33.04 ± 0.22	32.7[a]; 32.2[b]	33.5
Toluene	−31.62	7.57	39.20 ± 0.18	37.0[a]; 36.4[b]	36.6
Ethanol	−2.77	38.82	41.59 ± 0.15	38.9[d]; 40.8[b]	38.6
THF	−37.03	−5.57	31.46 ± 0.19	31.7[a] ; 30.6[d]	31.1
Acetonitrile	–23.52	9.49	33.01 ± 0.21	32.3[d]; 30.0[e]	–

[a] Diez et al. (2011).
[b] Dritsas et al. (2008).
[c] Vincent et al. (2012).
[d] Luo et al. (2019).
[e] Daubert and Danner (1985).
[f] Watson (1943).

and heterogeneity in the thickness of the polymer layer covering the support can distort the value of the weight of the polymer inside the column which is estimated from the ratio of the initial polymer/solvent mixture. Additionally, the friction of the particles of the impregnated support during preparation and loading of the column can generate debris or polymer powder, which can result in underestimation of the weight of the polymer in the column.

Theδ_P of SBR determined from the slope and the intercept of the curve of Fig. 5 revealed a value of 16.27 ± 0.12 MPa$^{0.5}$. The absence of data in the literature on the solubility parameter of SBR containing the same composition in comonomer units did not allow a rigorous comparison of our results with others, nevertheless the presence of data on the SBR with other compositions allows to give an idea on the real value of this parameter. Table 7 shows the solubility parameters of SBR containing different styrene/butadiene ratios determined by different methods.

As can be seen from these data, the value of the solubility parameter of SBR containing 30% styrene determined by viscosimetry seems to be closer to the value found in this work. On the other hand, that of SBR containing 40% styrene, determined by a swelling method, although the ratio of styrene unit in the copolymer is close to that used in this study, shows a higher value. The comparison of the two solubility parameters of the SBR containing the same styrene ratio (30%), one obtained by Diez et al using the PCIGC technique and the other by Ovejero using the viscosimetric method reveals significant deviation (∼5%).

3.2. Prediction of activity coefficients

3.2.1. Prediction using the non-random two-liquid (NRTL) model

The Flory–Huggins thermodynamic model expresses the relationship between the solvent activity, a_1, and the interaction parameter, $\chi_{1,p}$, as expressed by Eq. (20) (Flory, 1941):

$$lna_1 = \ln\frac{P}{P_1^o} = ln(1-\phi_2) + \left(1-\frac{1}{r}\right)\phi_2 + \chi_{ip}{\phi_2}^2, \tag{20}$$

where P and P_1^o are the vapor pressure of the solvent in the polymer solution and that of the pure solvent, respectively, and ϕ_2 is the volume fraction of the polymer.

We used this model to calculate the experimental equilibrium data of polymer–solvent solutions according to a previously described method (Ovejero et al., 2009). Estimation of P-xy values was possible using the polymer–solvent interaction parameters determined at a given temperature from these IGC experiments. Using the experimental values of $\chi_{1,p}$ and the hypothesis that the vapor pressure of a polymer is zero, we obtained the nonlinear fit of the NRTL model according to Eq. (21) (Renon and Prausnitz, 1968) using the Solver tool in Microsoft Excel software (Microsoft Corp., Redmond, WA, USA). We then adjusted the parameters of the NRTL equation ($\tau_{12}, \tau_{21}, G_{12}$, and$G_{21}$) and maintained $\alpha_{12} = 0.3$, which is ideal for nonpolar mixtures.

$$Ln\left(\Omega_1^{\infty}\right)_{NRTL} = x_2^2\left[\tau_{21}\left(\frac{G_{12}}{x_1 + x_2 G_{21}}\right)^2 + \frac{\tau_{12}G_{12}}{\left(x_1 G_{12} + x_2\right)^2}\right], \tag{21}$$

where $G_{12} = \exp\left(-\alpha_{12}\tau_{12}\right); G_{21} = \exp\left(-\alpha_{12}\tau_{21}\right)$.

Table 8 shows the experimental values of $\Omega_{1(IGC)}^{\infty}$ obtained from the IGC measurements and those obtained from the regression of the estimated P-xy data ($\Omega_{1(NRTL)}^{\infty}$). In all the cases, we obtained a residual root-mean square error of < 4.67%, indicating a very good fit for the NRTL model.

3.2.2. Prediction using the universal quasichemical (UNIQUAC) model

The estimated P-xy was also fitted to the UNIQUAC model according to Eq. (22) (Prausnitz et al., 1999) using the Solver tool in the Microsoft Excel software (Microsoft Corp.):

$$ln\left(\Omega_1^{\infty}\right)_{UNIQUAC} = x_i ln\frac{\phi_i}{x_i} + \frac{Z}{2}q_i ln\frac{\Theta_i}{\phi_i} + \phi_P\left(l_i - l_P\frac{r_i}{r_P}\right) - q_i ln\left(\Theta_i - \Theta_P\tau_{Pi}\right)$$

Table 6 Solubility parameters of solutes deducted at 30 °C and their comparison with those obtained by PCIGC and other methods; *Conversion 1 $MPa^{0.5}$ = 2.0455 $Cal^{0.5}$•$cm^{-1.5}$.

Solvent	δ_1 $(MPa)^{0.5}$*		
	This work	PCIGC	Other methods
n-Hexane	14.27 ± 0.12	14.90[a]; 14.80[b]; 10.83[c];14.90[d]; 15.35[e];14.81[g]	14.93[m]; 14.87[n]; 14.81[p]
n-Heptane	14.39 ± 0.18	13.70[a]; 11.82[c]; 15.2[e]; 15.30[d]; 15.30[f]; 15.18[g]	15.24[m]; 15.34[n]
n-Octane	13.66 ± 0.15	11.80[a]; 15.40[b]; 15.6[g]; 15.50[d]; 15.70[f]; 15.44[g]	15.42[n]
Cyclopentane	18.03 ± 0.18	12.28[c]; 16.6[h]; 13.89[i]; 16.40[f]; 16.56[g]	16.57[n]
Cyclohexane	16.76 ± 0.14	16.70[b]; 13.34[c]; 16.80[g];16.80[f]; 16.73[g]	16.77[m];16.73[n]; 16.73[p]
Benzene	18.44 ± 0.13	19.60[a]; 18.70[b]; 18.80[g];18.40[f]; 18.72[g]; 18.82[e]	18.72[m]; 18.45[n]; 18.72[p]
Toluene	17.52 ± 0.15	17.80[a]; 14.93[c]; 18.20[j];18.23[g]; 18.20[q]	18.20[m]; 18.21[n]; 18.23[p]
Ethanol	22.80 ± 0.12	23.00[a]; 23.01[h]; 26.52[i]; 26.19[e]; 26.10[q]	26.55[n]; 26.52[l]
THF	19.35 ± 0.10	19.50[a]; 19.46[l]; 16.18[f],	19.47[n]; 16.80[l]
Acetonitrile	24.10 ± 0.11	24.40[l]; 24.4[d]; 24.96[e]; 24.60[d]; 24.96[e]; 24.80[q]	24.43[n]; 24.34[p]

[k] Vay et al. (2011).
[a] Lim et al. (2014).
[b] Smith (1950).
[c] Sreekanth et al. (2012).
[d] DiPaola-Baranyi (1982).
[e] Jackson et al. (1994).
[f] Zhu et al. (2019).
[g] Ghosh (1971).
[h] Morales and Acosta (1996).
[i] Sreekanth and Reddy (2008).
[j] Ni et al. (2016).
[l] Adamska et al. (2020).
[m] Scott and Magat (1949).
[n] Koenhen and Smolders (1975).
[p] Hansen (1967).
[q] Adamska and Voelkel (2005).

$$+\Theta_P q_i\left(\frac{\tau_{Pi}}{\Theta_i-\Theta_P\tau_{Pi}}-\frac{\tau_{iP}}{\Theta_M+\Theta_i\tau_{iP}}\right), \tag{22}$$

where Z is the coordination number, which is assumed to be equal to 10. Additionally, q_i and r_i are the relative molecular surface area and relative molecular Van Der Waals volume for pure solvent, i, respectively. These values were calculated using the group-contribution method (Reid et al., 1987), and l_i was calculated from q_i and r_i values using Eq. (23):

$$l_i=\frac{Z}{2}(r_i-q_i)-(r_i-1). \tag{23}$$

For a polymer, r_P and q_P can also be calculated using the group-contribution method (Reid et al., 1987). ϕ_i and Θ_i are the volume and surface fractions of solvent i, respectively. The value of Θ_i is calculated from ϕ_i using the following equation:

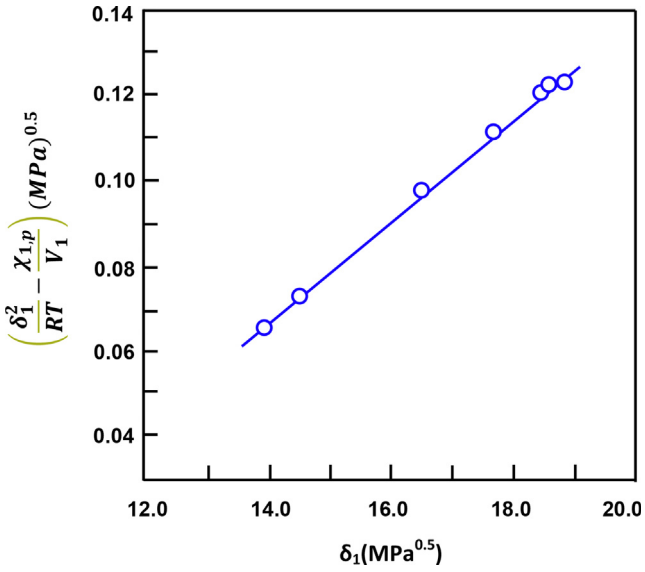

Fig. 5 Variation in $\delta_1^2/2 - (RT\chi_{1,p}/2V_1)$ with the solubility parameters of the solvents. Estimation of the solubility parameter of SBR.

Table 7 Comparative data of Hansen solubility parameters for SBR containing different compositions determined by IGC, swelling and viscosity measurements taken from the literature.

SBR composition styrene (%)	δ_p ($Mpa^{0.5}$)	Method	Ref.
60	17.73	Swelling measurement	Scott and Maya (1949)
40	17.50	–	Brandrup et al. (1999)
40	17.79	Swelling measurement	Scott and Maya (1949)
25	17.59	Swelling measurement	Scott and Maya (1949)
30 triblock	17.60	PCIGC	Diez et al. (2011)
30 triblock	16.70	Viscosity measurement	Ovejero (2010)
31triblock	17.60*	PCIGC	Romdhane et al. (1992)
45	16.27	CCIGC	This work

* Obtained at 35 °C.

$$\Theta_i=\frac{\Theta_i(q_i/r_i)}{\sum\Theta_i(q_i/r_i)}, \tag{24}$$

where τ_{iP} and τ_{Pi} are adjustable parameters and fitted using nonlinear regression on the P-xy data. The activity coefficients for all of the solvents determined at different temperatures using the UNIQUAC model ($\Omega^{\infty}_{1(UNIQUAC)}$) are listed in Table 8 along with those obtained by IGC ($\Omega^{\infty}_{1(IGC)}$) for comparison. In this model, we obtained a residual root-mean square error of 9.79%.

Table 8 Experimental values of the activity coefficient $\Omega^{\infty}_{1(IGC)}$ and $\Omega^{\infty}_{1(UNIQUAC)}$ obtained with non-linear regression.

Temperature	30 °C		40 °C		50 °C		60 °C		70 °C	
	Ω_1^{∞}		Ω_1^{∞}		Ω_1^{∞}		Ω_1^{∞}		Ω_1^{∞}	
	CAL[a]	EXP[b]	CAL[a]	EXP[b]	CAL[a]	EXP[b]	CAL[a]	EXP[b]	CAL[a]	EXP[b]
n-Hexane	6.30	7.23	6.24	7.16	6.20	7.12	6.35	7.28	6.43	7.38
n-Heptane	7.08	7.63	7.02	7.56	7.56	8.15	7.42	8.01	7.62	8.22
n-Octane	7.80	8.26	7.88	8.34	804	8.52	8.27	8.76	8.51	9.02
Cyclopentane	5.12	4.88	5.06	4.82	5.25	5.01	5.21	4.97	5.38	5.13
Cyclohexane	4.98	5.51	4.91	5.31	5.09	5.63	5.22	5.78	5.52	6.12
Benzene	5.98	4.89	5.82	4.76	5.65	4.62	5.45	4.45	5.36	4.38
Toluene	5.43	4.54	5.42	4.53	5.50	4.60	5.25	4.38	5.10	4.25
Ethanol	132.40	110.30	108.24	91.23	67.63	58.19	48.81	42.53	32.34	28.52
THF	5.86	4.58	6.35	4.98	6.56	5.15	6.86	5.39	7.02	5.52
Acetonitrile	–	62.18	–	56.85	–	51.07	–	45.32	–	40.38

[a] CAL: UNIQUAC.
[b] EXP: CCIGC.

4. Conclusion

In summary, we demonstrated successful determination of the thermodynamic parameters of SBR using a capillary column filled with a thin layer of SBR, followed by investigation of both polar and nonpolar solvents using CCIGC. The obtained solubility parameter of the SBR–solvent system was consistent with those previously determined and using different techniques. Comparison of the solubility parameters and the heats of vaporization of the investigated molecules with those obtained by PCIGC using different stationary phases revealed in the most studied molecules similar values. The gap observed between some values of the solubility parameters and the heat of vaporization obtained by CCIGC and those reported in the literature or between those of the same PCIGC method obtained by different authors seems to be due to the experimental errors occurred during the support traitement and/or the column preparation.

Furthermore, comparison of the activity coefficients of the solvents at ID and obtained by CCIGC with those obtained by fitting the NRTL and UNIQUAC models revealed excellent correlation. These results demonstrated the increased reliability of the CCIGC technique, as well as its speed and accuracy, relative to similar methods that use packed columns containing supports impregnated by the polymer. Moreover, use of the proposed method completely eliminated side effects related to the support.

Declaration of Competing Interest

The authors declare that they have no known competing financial interests or personal relationships that could have appeared to influence the work reported in this paper.

Acknowledgments

The authors gratefully acknowledge Mr. Kamal Chanane for performing all of the mathematical calculations.

Funding

This study was funded by the Deanship of Scientific Research, King Saud University (Research Group No. RGP-VPP-025).

References

Abd-El-Messieh, S., Abd-El-Nour, K., 2003. Effect of curing time and sulfur content on the dielectric relaxation of styrene butadiene rubber. J. Appl. Polym. Sci. 88, 1613–1621.

Adamska, K., Voelkel, A., 2005. Inverse gas chromatographic determination of solubility parameters of excipients. Int. J. Pharm. 304, 11–17.

Adamska, K., Voelkel, A., Sandomierski, M., 2020. Characterization of mesoporous aluminosilicate materials by means of inverse liquid chromatography. J. Chromatogr. A 1610, 460544.

Al-Ghait, M.K., Al-Arifi, A.S., Al Andis, N.M., AlOthman, Z.A., Aouak, T., 2012. Miscibility enhancement on the poly (vinylchloride)/poly (methylmethacrylate) blend and characterization by inverse gas chromatography: The corrected polymer–polymer interaction parameters from the probes dependency. J. Appl. Polym. Sci. 124, 1464–1474.

Balashova, I.M., Buduen, R.G., Danner, R.P., 2012. Solubility of organic solvents in 1, 4-cis-polybutadiene. Fluid Phase Equilib. 334, 10–14.

Balashova, I.M., Danner, R.P., Puri, P.S., Duda, J.L., 2001. Solubility and diffusivity of solvents and nonsolvents in polysulfone and polyetherimide. Ind. Eng. Chem. Res. 40, 3058–3064.

Benguergoura, H., Moulay, S., 2012. Styrene–butadiene rubber membranes for the pervaporative separation of benzene/cyclohexane mixtures. J. Appl. Polym. Sci. 123, 1455–1467.

Blanks, R.F., Prausnitz, J., 1964. Thermodynamics of polymer solubility in polar and nonpolar systems. Ind. Eng. Chem. Fundam. 3, 1–8.

Bonifaci, L., Carnelli, L., Cori, L., 1994. Determination of infinite dilution diffusion and activity coefficients of solvents in polystyrene by inverse gas chromatography on a capillary column. J. Appl. Polym. Sci. 51, 1923–1930.

Boublík, T., Fried, V., Hála, E., 1984. The vapour pressures of pure substances.

Brandrup, J., Immergut, E., Grulke, E., 1999. Polymer Handbook. John & Wiley Sons. Inc., New York, pp. 171–186.

Cai, W., Ramesh, N., Tihminlioglu, F., Danner, R.P., Duda, J.L., DèHaan, A., 2002. Phase equilibrium and diffusion of solvents in polybutadiene: A capillary-column inverse gas chromatography study. J. Polym. Sci., Part B: Polym. Phys. 40, 1046–1055.

Chahal, R.P., Mahendia, S., Tomar, A., Kumar, S., 2012. γ-Irradiated PVA/Ag nanocomposite films: Materials for optical applications. J. Alloy. Compd. 538, 212–219.

Cho, K., Jang, W.J., Lee, D., Chun, H., Chang, Y.-W., 2000. Fatigue crack growth of elastomers in the swollen state. Polymer 41, 179–183.

Conder, J., Young, C., 1979. Physicochemical Measurements by Gas Chromatography. Willey, NY.

Daubert, T.E., Danner, R.P., 1985. Data compilation tables of properties of pure compounds. Design Institute for Physical Property Data, American Institute of Chemical . . ..

Davis, P.K., Danner, R.P., Duda, J.L., Hadj Romdhane, I., 2004. Use of inverse gas chromatography to study binary polymer– solvent systems near the glass transition temperature. Macromolecules 37, 9201–9210.

Diez, E., Ovejero, G., Romero, M., Diaz, I., 2011. Polymer–solvent interaction parameters of SBS rubbers by inverse gas chromatography measurements. Fluid Phase Equilib. 308, 107–113.

DiPaola-Baranyi, G., 1982. Estimation of polymer solubility parameters by inverse gas chromatography. Macromolecules 15, 622–624.

Domínguez, J.A.G., Díez-Masa, J.C., Davankov, V., 2001. Retention parameters in chromatography. Pure Appl. Chem. 73, 969–992.

Dritsas, G., Karatasos, K., Panayiotou, C., 2008. Investigation of thermodynamic properties of hyperbranched poly (ester amide) by inverse gas chromatography. J. Polym. Sci., Part B: Polym. Phys. 46, 2166–2172.

Eser, H., Tihminlioglu, F., 2005. Solubility and diffusivity of solvents and nonsolvents in poly (methyl methacrylate co butyl methacrylate). Fluid Phase Equilib. 237, 68–76.

Etxeberria, A., Uriarte, C., Fernandez-Berridi, M., Iruin, J., 1994. Probing polymer-polymer interaction parameters in miscible blends by inverse gas chromatography: solvent effects. Macromolecules 27, 1245–1248.

Farshchi, N., Abbasian, A., Larijani, K., 2018. Assessment of the thermodynamic properties of DL-p-mentha-1, 8-diene, 4-isopropyl-1-methylcyclohexene (DL-limonene) by inverse gas chromatography (IGC). J. Chromatogr. Sci. 56, 671–678.

Flory, P.J., 1941. Thermodynamics of high polymer solutions. J. Chem. Phys. 9, 660.

George, S.C., Ninan, K.a., Thomas, S., 1999. Effect of degree of crosslinking on swelling and mechanical behaviour of conventionally vulcanised styrene-butadiene rubber membranes. Polym. Polym. Compos. 7, 343–353.

Ghosh, S., 1971. Solubility parameter and hydrocarbon sorption of low density polyethylene. Die Makromolekulare Chemie: Macromolecular Chemistry and Physics 143, 181–187.

Gray, D., Guillet, J., 1973. Studies of diffusion in polymers by gas chromatography. Macromolecules 6, 223–227.

Guggenheim, E., Wormald, C., 1965. Systematic deviations from the principle of corresponding states. J. Chem. Phys. 42, 3775–3780.

Guillet, J., Al-Saigh, Z.Y., 2006. Inverse gas chromatography in analysis of polymers. Encyclopedia of Analytical Chemistry: Applications, Theory and Instrumentation.

Hadj-Ziane, A., Moulay, S., Canselier, J.P., 2005. Use of inverse gas chromatography to account for the pervaporation performance in the microemulsion breakdown. J. Chromatogr. A 1091, 145–151.

Hansen, C., 1967. Three dimensional solubility parameter and solvent diffusion coefficient. Importance in surface coating formulation. Doctoral Dissertation.

Horta, A., Pastoriza, M.A., 2005. The interaction parameter of crosslinked networks and star polymers. Eur. Polym. J. 41, 2793–2802.

Huang, J.-C., 2006. Anomalous solubility parameter and probe dependency of polymer–polymer interaction parameter in inverse gas chromatography. Eur. Polym. J. 42, 1000–1007.

Huang, J.C., 2004. Methods to determine solubility parameters of polymers at high temperature using inverse gas chromatography. J. Appl. Polym. Sci. 94, 1547–1555.

Jackson, P.L., Huglin, M.B., Cervenka, A., 1994. Use of inverse gas chromatography to quantify interactions in anhydride cured epoxy resins. Polym. Int. 35, 135–143.

James, A.T., Martin, A.J., 1952. Gas-liquid partition chromatography: the separation and micro-estimation of volatile fatty acids from formic acid to dodecanoic acid. Biochem. J 50, 679–690.

Kim, K.K., Yeon, J., Lee, H.J., Yeon, J.H., 2019. Dimensional stability of SBR-modified cementitious mixtures for use in 3D additive construction. Appl. Sci. 9, 3386.

Koenhen, D., Smolders, C., 1975. The determination of solubility parameters of solvents and polymers by means of correlations with other physical quantities. J. Appl. Polym. Sci. 19, 1163–1179.

Laub, R.J., Pecsok, R.L., 1978. Physicochemical applications of gas chromatography. Wiley.

Lim, H.J., Lee, K., Cho, Y.S., Kim, Y.S., Kim, T., Park, C.R., 2014. Experimental consideration of the Hansen solubility parameters of as-produced multi-walled carbon nanotubes by inverse gas chromatography. PCCP 16, 17466–17472.

Luo, Y., Liu, H., Xiang, B., Chen, X., Yang, W., Luo, Z., 2019. Temperature dependence of the interfacial bonding characteristics of silica/styrene butadiene rubber composites: a molecular dynamics simulation study. RSC Adv. 9, 40062–40071.

Marzocca, A., 2007. Evaluation of the polymer–solvent interaction parameter χ for the system cured styrene butadiene rubber and toluene. Eur. Polym. J. 43, 2682–2689.

Mohammadi-Jam, S., Waters, K., 2014. Inverse gas chromatography applications: A review. Adv. Colloid Interface Sci. 212, 21–44.

Morales, E., Acosta, J.L., 1996. Polymer solubility parameters of poly (propylene oxide) rubber from inverse gas chromatography measurements. Polym. J. 28, 127–130.

Moulay, S., Benguergoura, H., Aouak, T., 2006. Use of inverse gas chromatography to account for the pervaporation performance in monitoring the oxidation of primary alcohols. J. Chromatogr. A 1135, 78–84.

Ni, H., Ren, S., Fang, G., Ma, Y., 2016. Determination of alkali lignin solubility parameters by inverse gas chromatography and Hansen solubility parameters. BioResources 11, 4353–4368.

Ovejero, G., Romero, M., Diez, E., Díaz, I., 2010. Thermodynamic interactions of three SBS (styrene–butadiene–styrene) triblock copolymers with different solvents, by means of intrinsic viscosity measurements. Eur. Polym. J. 46, 2261–2268.

Ovejero, G., Romero, M.D., Díez, E., Díaz, I., Pérez, P., 2009. Thermodynamic modeling and simulation of styrene– butadiene rubbers (SBR) solvent equilibrium staged processes. Ind. Eng. Chem. Res. 48, 7713–7723.

Pawlisch, C.A., Bric, J.R., Laurence, R.L., 1988. Solute diffusion in polymers. 2. Fourier estimation of capillary column inverse gas chromatography data. Macromolecules 21, 1685–1698.

Pawlisch, C.A., Macris, A., Laurence, R.L., 1987. Solute diffusion in polymers. 1. The use of capillary column inverse gas chromatography. Macromolecules 20, 1564–1578.

Prausnitz, J., Lichtenthaler, R., Azevedo, E., 1999. Molecular Thermodynamics of Fluid Phase Equilibria. Prentice Hall PTR, Englewood Cliffs.

Reid, R.C., Prausnitz, J.M., Poling, B.E., 1987. The properties of gases and liquids.

Renon, H., Prausnitz, J.M., 1968. Local compositions in thermodynamic excess functions for liquid mixtures. AIChE J. 14, 135–144.

Romdhane, I.H., Plana, A., Hwang, S., Danner, R., 1992. Thermodynamic interactions of solvents with styrene–butadiene–styrene triblock copolymers. J. Appl. Polym. Sci. 45, 2049–2056.

Scott, R.L., Magat, M., 1949. Thermodynamics of high-polymer solutions. III. Swelling of cross-linked rubber. J. Polym. Sci. 4, 555–571.

Scuracchio, C., Bretas, R., Isayev, A.I., 2004. Blends of PS with SBR devulcanized by ultrasound: Rheology and morphology. J. Elastomers Plast. 36, 45–75.

Smith, J.M., 1950. Introduction to chemical engineering thermodynamics. ACS Publications.

Sreekanth, T., Ramanaiah, S., Lee, K.D., Reddy, K., 2012. Hansen solubility parameters in the analysis of solvent–solvent interactions by inverse gas chromatography. J. Macromol. Sci., Part B 51, 1256–1266.

Sreekanth, T., Reddy, K., 2008. Evaluation of solubility parameters for nonvolatile branched hydrocarbons by inverse gas chromatography. J. Appl. Polym. Sci. 108, 1761–1769.

Tihminlioglu, F., Danner, R.P., 1999. Application of inverse gas chromatography to the measurement of diffusion and phase equilibria in polyacrylate–solvent systems. J. Chromatogr. A 845, 93–101.

Traeger, R.K., Castonguay, T.T., 1966. Effect of γ-radiation on the dynamic mechanical properties of styrene–butadiene rubbers. J. Appl. Polym. Sci. 10, 491–509.

Ugraskan, V., Isik, B., Yazici, O., Cakar, F., 2020. Thermodynamic characterization of sodium alginate by inverse gas chromatography. J. Chem. Eng. Data 65, 1795–1801.

Vay, K., Scheler, S., Frieß, W., 2011. Application of Hansen solubility parameters for understanding and prediction of drug distribution in microspheres. Int. J. Pharm. 416, 202–209.

Voelkel, A., Fall, J., 1995. The use of the Flory-Huggins interaction parameter for the characterization of vacuum distillation residue fractions of mineral oils. Chromatographia 41, 414–418.

Voelkel, A., Strzemiecka, B., Adamska, K., Milczewska, K., 2009. Inverse gas chromatography as a source of physiochemical data. J. Chromatogr. A 1216, 1551–1566.

Watson, K., 1943. Thermodynamics of the liquid state. Ind. Eng. Chem. 35, 398–406.

Yampolskii, Y., Belov, N., 2015. Investigation of polymers by inverse gas chromatography. Macromolecules 48, 6751–6767.

Zhu, Q.-N., Wang, Q., Hu, Y.-B., Abliz, X., 2019. Practical determination of the solubility parameters of 1-alkyl-3-methylimidazolium bromide ([CnC1im] Br, n = 5, 6, 7, 8) ionic liquids by inverse gas chromatography and the Hansen solubility parameter. Molecules 24, 1346.